RESEARCH ARTICLE OPEN ACCESS

Heat And Mass Transfer In Non-Newtonian Nanofluid Flow From A Vertical Melting Front

D.Rajani[1], K.Hemalatha[2], J.Siva Ramprasad[3]

[1, 2, 3] Department of Mathematics, V.R. Siddhartha Engineering College, Vijayawada – 520007.
[1]Research Scholar, Krishna University, Machilipatnam-521001.

ABSTRACT: In present work, the problem of convective boundary layer flow of a warm laminar non-Newtonian nanofluid over a vertical surface with melting effect is studied numerically. A non-Newtonian fluid is one whose stream bend is nonlinear. The relationship between shear stress and shear rate for this type of fluid can be mathematically expressed as $\tau_{yx} = K(\dot{\gamma}_{yx})^n$,so the apparent viscosity for the power law fluid is $\mu = K(\dot{\gamma}_{yx})^{n-1}$. The fluid display diverse properties, shear-thinning, Newtonian behaviour, shear thickening for different values of power law index. A nanofluid model is employed to incorporate the effects of brownian motion and thermophoresis. The governing set of partial differential equations was non-dimensionalized and reduced to a set of ordinary differential equations and is then solved numerically using Matlab. Numerical results for surface heat transfer rate and mass transfer rate are studied in the presence of different physical parameters and are presented graphically.

Keywords: Melting, Non-Newtonian Nanofluid ,Heat transfer.

NOMENCLATURE

(x , y) Cartesian coordinates
$(u. v)$ velocity components along in the vertical (x) and horizontal (y) directions,
Nr buoyancy ratio parameter
Nb brownian motion parameter
D_B brownian motion coefficient
Nt thermophoresis parameter
D_T thermophoretic diffusion coefficient
Sh_x local sherwood number
Ra_x local Rayleigh number
Gr^* Grashof number
M melting parameter
Le Lewis number
K modified permeability of the porous medium
g gravitational acceleration
T local temperature
C nanoparticle volume fraction
k effective thermal conductivity of the porous medium

Greek symbols

β volumetric expansion of the base fluid
α_m thermal diffusivity of the porous medium
ρf_∞ density of the base fluid
ρ_p density of nanoparticle
$(\rho c)_f$ heat capacity of the nanofluid
$(\rho c)_p$ effective heat capacity of the nanoparticle material.
θ dimensionless temperature
ϕ dimensionless concentration
τ ratio of the effective heat capacity of the nanoparticle material and the heat capacity of the fluid
ε porosity of the porous medium
μ consistency index of the power law fluid
ψ stream function
C_f specific heat of convective fluid
C_{sf} specific heat of solid liquid phase
h_{sf} latent heat of melting of solid

Subscripts

m = melting point
∞ = condition at infinity

I. INTRODUCTION

Recently the study of non-Newtonian nanofluids has received much attention due to its applications in manufacturing and industry technologies. Classical heat transfer fluids such as water, ethylene glycol, and engine oil have a some limitation in heat transfer efficiency. Metals are very good conductivities. To overcome this disadvantage of fluids, it would be desired to combine metals and fluids to produce a heat transfer medium. Numerous intriguing uses of non-Newtonian power law fluids with yield stress on convective heat transport in fluid saturated porous media considering geothermal applications and oil reservoir engineering applications was presented by Shenoy [1]. Ellahi et al. [2] have expounded that non-Newtonian nanofluids have potential roles in physiological transport as biological solutions and also in polymer melts, paints etc..

The effect of melting and nanofluid flow over a vertical plate has been investigated by several researchers due to its wide range of applications. Hady et al. [3] studied boundary layer phenomena on non-Newtonian flow over a vertical plate in porous medium saturated with nanofluid. They observed that nanoparticle volume fraction decreases with an increase in Le and n. Kumari and Gorla [4] studied the effect of melting on mixed convective boundary layer flow over a vertical plate embedded in a porous medium saturated with a Nanofluid. In their studies they found that melting phenomenon increases the heat transfer rate at the solid interface. The effects of melting heat transfer in a nanofluid flow past a permeable continuous moving surface was studied by Gorla et al. [5] They observed that as melting parameter increases the velocity profile increases, whereas the temperature and concentration profiles decreases. Kairi and Ram Reddy [6] explored the effects of melting on mixed convective heat and mass transfer in non-Newtonian nanofluid saturated in porous medium. Their findings indicates that Nusselt and Sherwood number decrease with increase of melting parameter for both pseudo plastic and dilatants fluids.

The main desire of the commenced inquire is to interpret the effects of melting in non-Newtonian nanofluid over a vertical plate. Most reviews published in the literature have not considered the melting effect on non-Newtonian nanofluid flow over a vertical surface. Numerical solutions for various parameters are represented graphically.

II. MATHEMATICAL ANALYSIS

In this work we consider melting effects steady two-dimensional boundary layer non-Newtonian nanofluid flow over a vertical surface in a porous medium. Further we consider a Cartesian coordinate system (x, y),where x and y are coordinates measured along the plate and normal to it, respectively. It is assumed that this plate constitutes the interface between the liquid and solid phases during the melting inside the porous matrix. The plate temperature is T_m, which is constant and the liquid phase temperature $T_\infty$and temperature of the solid far from the interface is T_s. Nanoparticle fraction C to be taken as constant values C_w and C_∞ respectively. Based on the above suppositions, the governing equations for steady laminar flow heat and mass transfer can be composed as follows

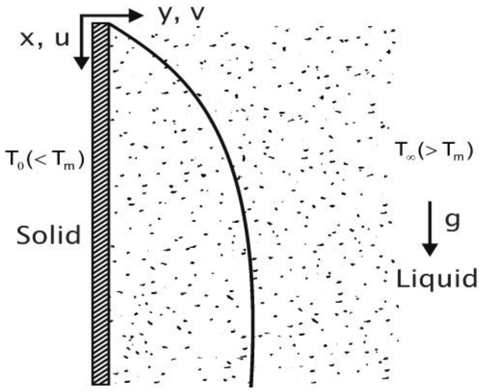

Fig 1. Physical model of a problem

$$\frac{\partial u}{\partial x}+\frac{\partial v}{\partial y}=0 \quad (1)$$

$$\frac{\partial u^n}{\partial y}+\rho f_\infty \frac{bk^*}{\mu}\frac{\partial u^2}{\partial y}=\frac{(1-C_\infty)Kg\beta\rho\, f_\infty}{\mu}\frac{\partial T}{\partial y}-\frac{(\rho_p-\rho f_\infty)Kg}{\mu}\frac{\partial C}{\partial y} \quad (2)$$

$$u\frac{\partial T}{\partial x}+v\frac{\partial T}{\partial y}=\alpha_m\frac{\partial^2 T}{\partial y^2}+\tau\left\{D_B\frac{\partial T}{\partial y}\frac{\partial C}{\partial y}+\frac{D_T}{T_\infty}\left(\frac{\partial T}{\partial y}\right)^2\right\} \quad (3)$$

$$\frac{1}{\varepsilon}\left(u\frac{\partial C}{\partial x}+v\frac{\partial C}{\partial y}\right)=D_B\frac{\partial^2 C}{\partial y^2}+\left(\frac{D_T}{D_\infty}\right)\frac{\partial^2 T}{\partial y^2} \quad (4)$$

where $\alpha_m=\frac{k}{(\rho c)_f}$ and $\tau=\frac{\varepsilon(\rho c)_p}{(\rho c)_f}$

The boundary conditions for equations (1)-(4) are given in the form

$$k\frac{\partial T}{\partial y}=\rho\left[h_{sf}+c_s(T_m-T_0)\right]v,\ T=T_m,\ C=C_w \text{ at } y=0$$

$$u\rightarrow 0, T=T_\infty, C\rightarrow C_\infty \text{ as } y\rightarrow\infty \quad (5)$$

Here u, v are the velocity components in the vertical (x) and horizontal (y) directions, n is the power law index, K is the modified permeability of the porous medium, g is the gravitational acceleration, β is the volumetric expansion of the base fluid, $\rho f_\infty$is the density of the base fluid, μ is the consistency index of the power law fluid, T is the local temperature, C is the nanoparticle volume fraction, $\rho_p$is the density of nanoparticle, τ is ratio of the effective heat capacity of the nanoparticle material and the heat capacity of the fluid, $D_B$is the Brownian motion coefficient, $D_T$is the thermophoretic diffusion coefficient, ε is the porosity of the porous medium respectively. k is the effective thermal conductivity of the porous medium, $(\rho c)_f$is the heat capacity of the nanofluid and $(\rho c)_p$is the effective heat capacity of the nanoparticle material.

The modified permeability of the porous medium K of the non - Newtonian power law fluid is defined as

$$K = \frac{1}{2c_t}\left(\frac{n\varepsilon}{3n+1}\right)^n\left(\frac{50k^*}{3\varepsilon}\right)^{\frac{n+1}{2}}$$

$$k^* = \frac{\varepsilon^3 d^2}{150(1-\varepsilon)^2}$$

and

$$c_t = \begin{cases} \frac{25}{12}\,(n=1) \\ \frac{2}{3}\left(\frac{8n}{9n+3}\right)^n\left(\frac{10n-3}{6n+1}\right)\left(\frac{75}{16}\right)^{\frac{3(10n-3)}{10n+11}}\,(n \neq 1) \end{cases}$$

The continuity equation (1) is satisfied by introducing a stream function $\psi(x,y)$ such that

$u = \frac{\partial\psi}{\partial y}$ and $v = -\frac{\partial\psi}{\partial x}$

where $\psi = \alpha_m Ra_x^{\frac{1}{2}} f(\eta), f(\eta)$ is the dimensionless stream function and $\eta = (y/x)Ra_x^{\frac{1}{2}}$ .The velocity components are given

$u = \left(\frac{\alpha_m}{x}\right) Ra_x f'(\eta)$ and

$$v = \left(\frac{\alpha_m}{2x}\right) Ra_x^{\frac{1}{2}}\left\{\frac{y}{x}Ra_x^{\frac{1}{2}} f'(\eta) - f(\eta)\right\} \quad (6)$$

where $Ra_x = \frac{x}{\alpha_m}\left(\frac{(1-C_\infty)Kg\beta\rho\, f_\infty\Delta T}{\mu}\right)^{\frac{1}{n}}$.

The temperature and concentration are represented as

$T = T_m + \Delta T\theta(\eta)$ and $C = C_\infty + \Delta C\phi(\eta)$ (7)

where $\theta(\eta)$ and $\phi(\eta)$ are the dimensionless temperature and dimensionless concentration. On using equation (5)and (6), equations (2) - (4) transform into the following two-point boundary value problem

$$(n(f')^{n-1} + 2Gr^* f')f'' - \theta' + Nr\phi' = 0, \quad (8)$$

$$\theta'' + \frac{1}{2}f\theta' + Nb\theta'\phi' + Nt\theta'^2 = 0, \quad (9)$$

$$\phi'' + \frac{1}{2}\mathrm{Le} f\phi' + \frac{\mathrm{Nt}}{\mathrm{Nb}}\theta'' = 0, \quad (10)$$

$$f(0) + 2M\theta'(0) = 0, f'(\infty) \to 0, \quad (11)$$

$$\theta(0) = 0, \theta(\infty) \to 1, \quad (12)$$

$$\phi(0) = 0, \phi(\infty) \to 1 \quad (13)$$

where the primes denote differentiation with respect to η. The non-dimensional constants in equations (8) - (10) are the Grashof number Gr^*, buoyancy ratio parameter Nr, coefficient of Brownian motion parameter Nb, thermophoresis parameter Nt, the Lewis number Le and the melting parameter M. These are defined as

$$Gr^* = b\left(\frac{\lfloor(1-C_\infty)g\beta\Delta T\rfloor^{2-n}K^2 pf_\infty^2}{\mu^2}\right)^{\frac{1}{n}},$$

$$Nr = \frac{(\rho_p - \rho_f)\Delta C}{(1-C_\infty)\beta\rho\, f_\infty\Delta T}, \quad Nb = \frac{\tau D_B\Delta C}{\alpha_m},$$

$$Nt = \frac{\tau D_T\Delta T}{\alpha_m T_\infty}, Le = \frac{\alpha_m}{\varepsilon D_B}, M = \frac{C_f(T_\infty - T_m)}{h_{sf} + C_{sf}(T_m - T_0)}$$

Heat and Mass transfer Coefficients

The local heat flux at the vertical wall is given by

$$q_w = -k\left[\frac{\partial T}{\partial y}\right]_{y=0} \quad (14)$$

The local Nusselt number is defined as

$$Nu_x = \frac{xq_w}{k(T_\infty - T_m)} \quad (15)$$

Where is the effective thermal conductvity of the porous medium, which is the sum of the molecular thermal conductivity and the dispersion thermal conductivity. Using equation in equation the dimensionless Nusselt number can be represented as below

$$\frac{Nu_x}{Ra_x^{\frac{1}{2}}} = -\theta'(0) \quad (16)$$

The mass flux at vertical wall is given by

$$q_m = -D_B\left[\frac{\partial C}{\partial y}\right]_{y=0} = -D_B\,(C_\infty - C_m)\frac{1}{x}Ra_x^{\frac{1}{2}}\phi'(0) \quad (17)$$

The local Sherwood is defined as

$$Sh_x = \frac{xq_m}{D_B(C_w - C_\infty)} \quad (18)$$

Using this the dimensionless Sherwood number obtained as

$$\frac{Sh_x}{Ra_x^{\frac{1}{2}}} = -\phi'(0) \quad (19)$$

Where $Ra_x = \frac{x}{\alpha_m}\left(\frac{(1-C_\infty)Kg\beta\rho\, f_\infty\Delta T}{\mu}\right)^{\frac{1}{n}}$ is the local Rayleigh number.

III. RESULTS AND DISCUSSION

Equations(8)-(10) were solved numerically along with the boundary conditions (11)-(13) for parametric values of Le (Lewis number), Nr (Buoyancy ratio number), Nb (Brownian motion parameter) and Nt (Thermophoresis parameter) using MatLab bvp4c. The results obtained were in good agreement with the previously published works.

Figure 2: Variation of velocity profiles with similarity variable η for (a) $Gr^* = 0$ (b) $Gr^* = 0.01$ and (c)$Gr^* = 1$, when $Nb = Nt = 0.3, Nr = 0.1$, $Le = 1$

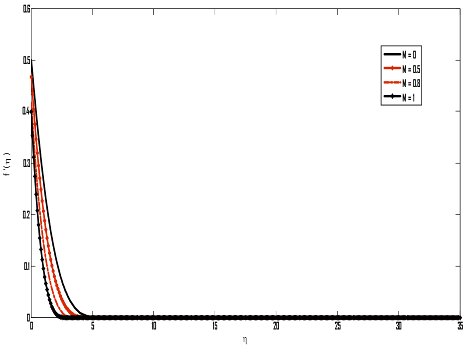

Fig 2(a)

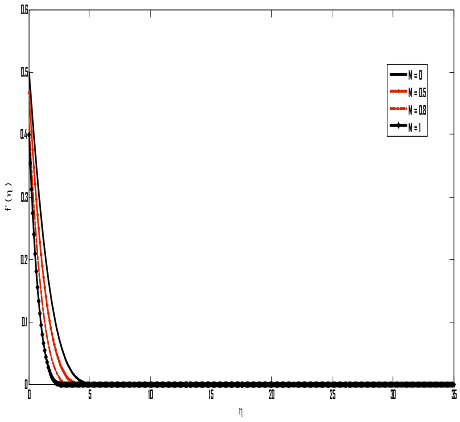

Fig 2(b)

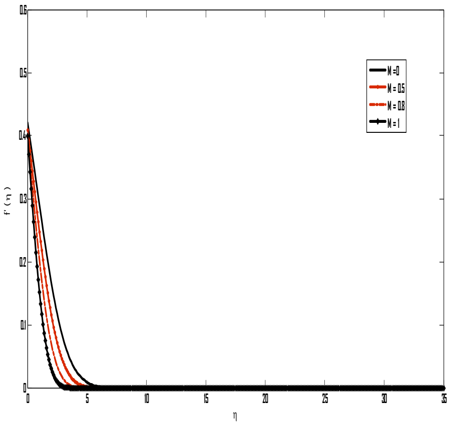

Fig 2(c)

Figure 3: Variation of velocity profiles with similarity variable η for (a) $Gr^* = 0$ (b) $Gr^* = 0.01$ and (c)$Gr^* = 1$,when $Nb = Nt = 0.3, Nr = -0.1$, $Le = 1$

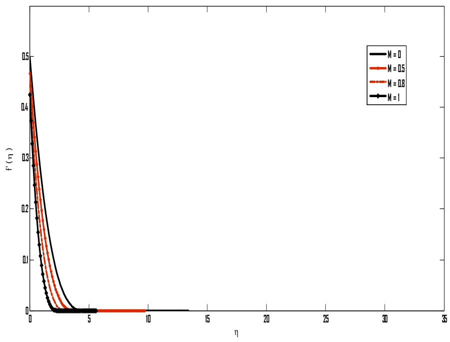

Fig 3(a)

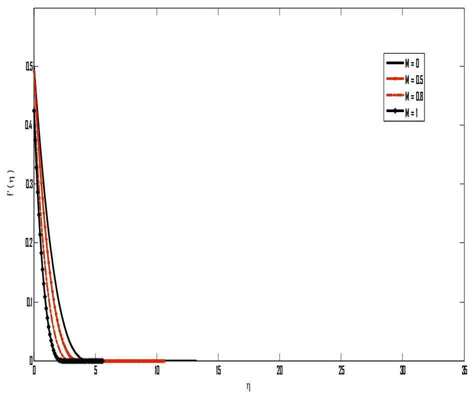

Fig 3(b)

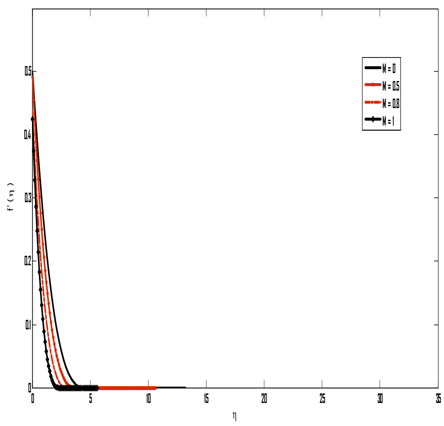

Fig 3(c)

Figure 4: Variation of temperature profiles with similarity variable η for (a) $Gr^* = 0$ (b) $Gr^* = 0.01$ and (c) $Gr^* = 1$, when $Nb = Nt = 0.3, Nr = 0.1$, $Le = 1$

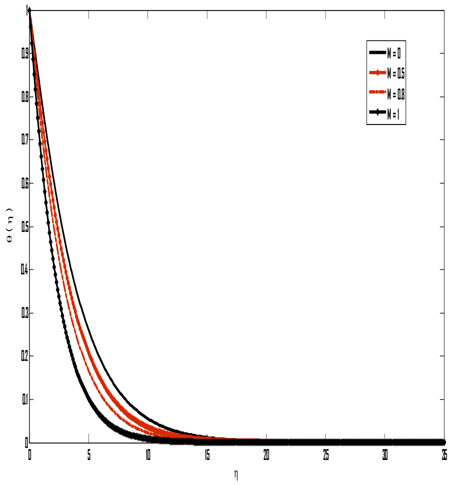

Fig 4(a)

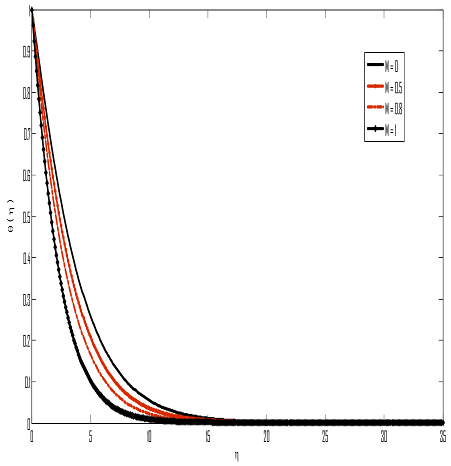

Fig 4(b)

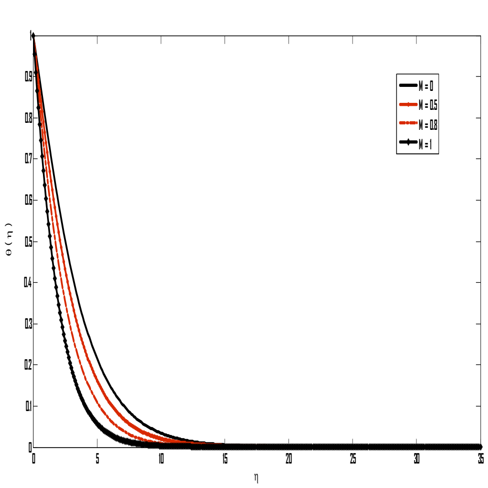

Fig 4(c)

Figure 5: Variation of temperature profiles with similarity variable η for (a) $Gr^* = 0$ (b) $Gr^* = 0.01$ and (c) $Gr^* = 1$, when $Nb = Nt = 0.3, Nr = -0.1$, $Le = 1$

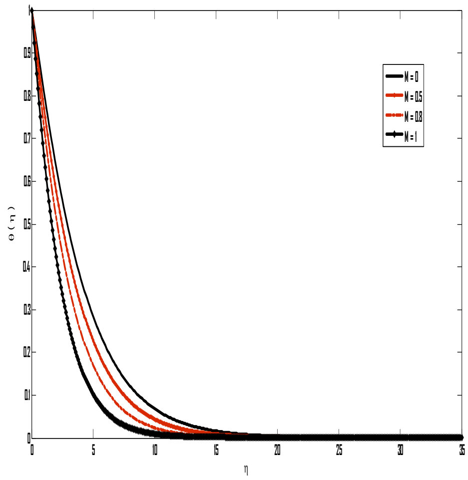

Fig 5(a)

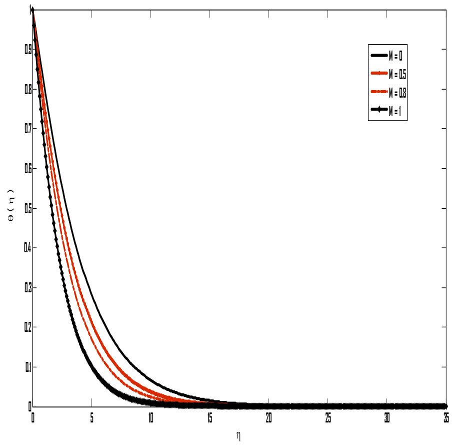

Fig 5(b)

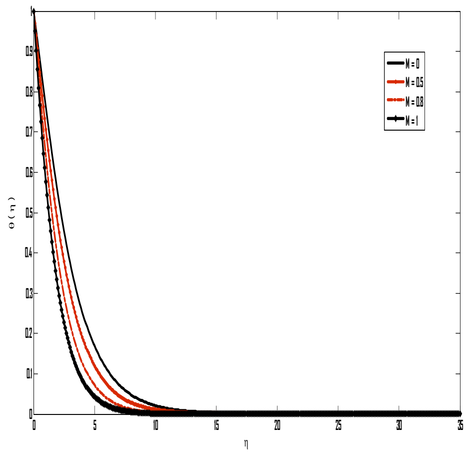

Fig 5(c)

Figure 6:Variation of concentration profiles with similarity variable η for (a) $Gr^* = 0$ (b) $Gr^* = 0.01$ and (c) $Gr^* = 1$,when $Nb = Nt = 0.3, Nr = 0.1$, $Le = 1$

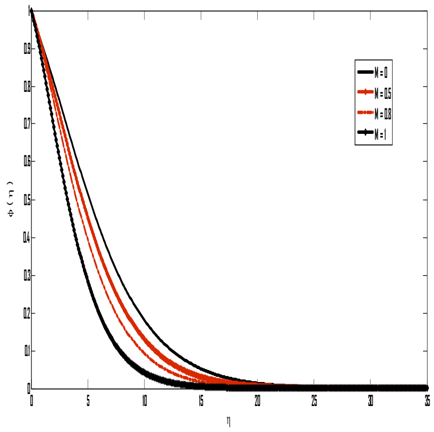

Fig 6(a)

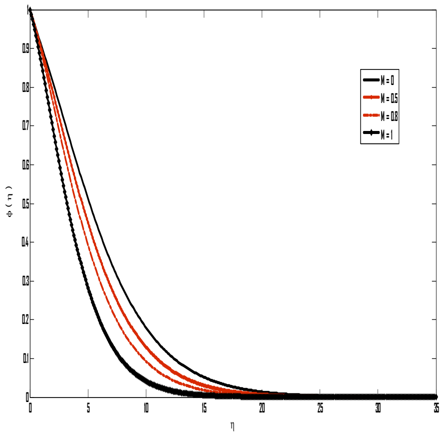

Fig 6(b)

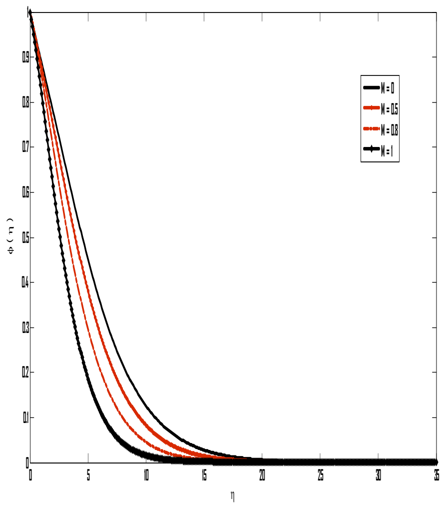

Fig 6(c)

Figure 7: Variation of concentration profiles with similarity variable η for (a) $Gr^* = 0$ (b) $Gr^* = 0.01$ and (c) $Gr^* = 1$,when $Nb = Nt = 0.3, Nr = -0.1$, $Le = 1$

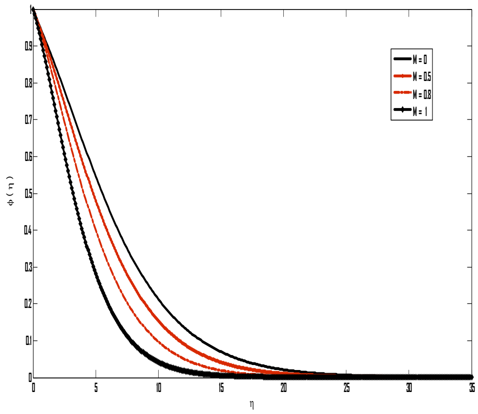

Fig 7(a)

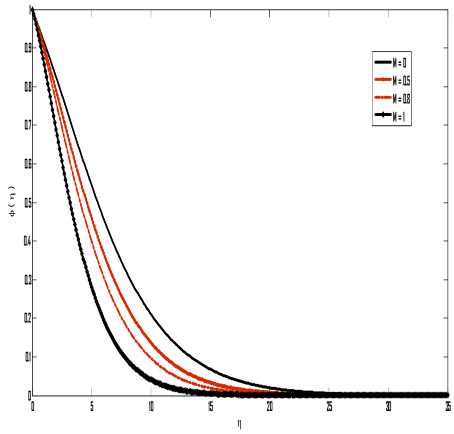

Fig 7(b)

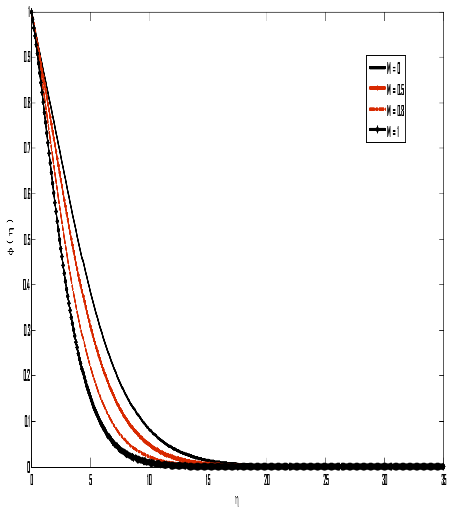

Fig 7(c)

Figures 2-7, display results for the variation in the velocity, temperature, concentration within the boundary layer for different values of Grashof number Gr^* with $Nb = Nt = 0.3$ and $Le = 1$. As the melting parameter M increases, the velocity, temperature and concentration decrease in both aiding and opposing cases.

Figure 8: Heat transfer coefficient as a function of melting parameter M for different values of Grashof number $Gr^*$when $n = 0.5, Nb = Nt = 0.3$, $Le = 1$, (a) $Nr = 0.1$ and (b) $Nr = -0.1$.

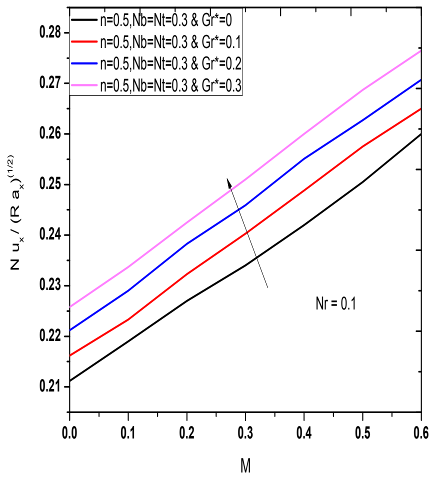

Fig 8(a)

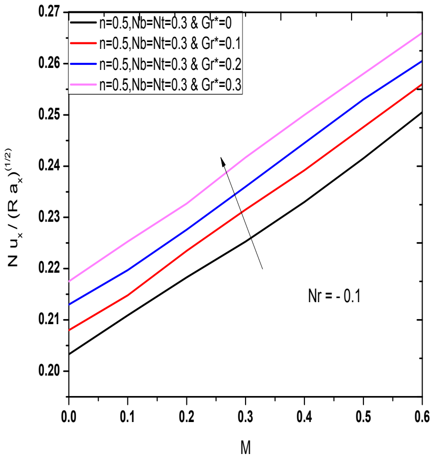

Fig 8(b)

In figure 8, it is observed that as Gr^* increases th heat transfer rate increases with melting parameter M for fixed $n = 0.5, Nb = Nt = 0.3$, in both aiding and opposing flows.

Figure 9: Mass transfer coefficient as a function of Lewis number Le for different values of M, when $Nr = 0.1, Nb = Nt = 0.3$, (a) $Gr^* = 0$ and (b) $Gr^* = 0.3$.

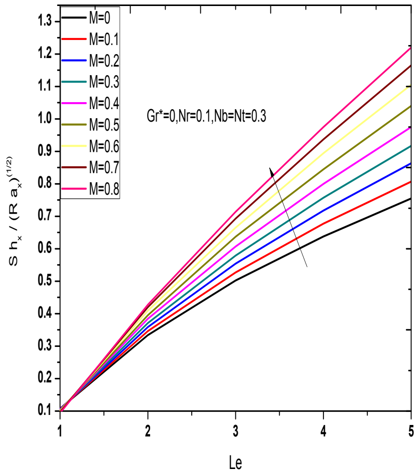

Fig 9(a)

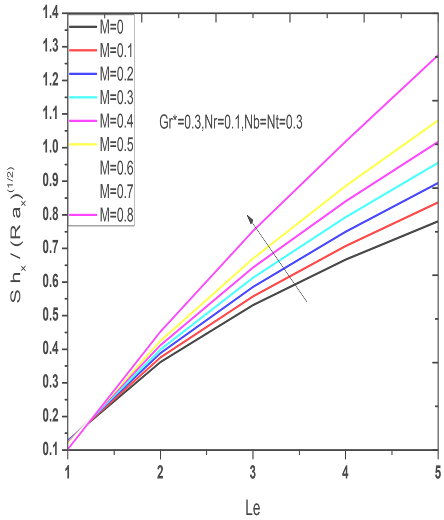

Fig 9(b)

From figure 9, It was observed that the mass transfer coefficient as a function of Lewis number Le increases with melting parameter M for $Nr = 0.1, Nb = Nt = 0.3$, in the presence and in the absence of Gr^*

Figure 10: Heat transfer coefficient as a function of melting parameter M for different values of Nr, when n=0.5, $\mathrm{Nb} = \mathrm{Nt} = 0.3$, for (a) $\mathrm{Gr}^* = 0$ and (b) $\mathrm{Gr}^* = 0.3$.

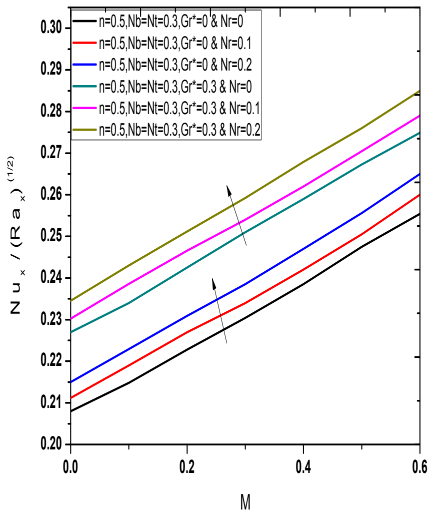

Fig 10

Figure 10 shows that the heat transfer coefficient increases as a function of melting parameter for different values of Nr for $\mathrm{Gr}^* = 0$ and $\mathrm{Gr}^* = 0.3$. But this increase is more for the increasing values of Grashof number Gr^*

IV. CONCLUSIONS

In this work, Numerical outcomes for surface heat and mass transfer rates have been presented for parametric variations in Melting parameter M, Buoyancy ratio parameter Nr, Brownian motion parameter Nb, Thermophoresis parameter Nt, Grashof number $\mathrm{Gr}^*$and Lewis number Le.

The results indicate that :

1. as Lewis number Le increases the heat and mass transfer rates increase.
2. as melting parameter M increases, the heat and mass transfer rates increase. Also it is observed that the melting phenomenon increases the heat transfer (Nusselt number) rate at the solid fluid interface.
3. as Grashof number Gr^* increases, velocity , temperature and nanoparticle concentration profiles decreases.
4. as Grashof number Gr^* increases, heat transfer coefficient increases for different values of Nr

V.REFERENCES

[1]. A.V. Shenoy, Non-Newtonian fluid heat transfer in porous media. Adv. Heat Transf., 24 (1994) 101 -190.

[2]. R. Ellahi, M. Raza, K. Vafai, Series solutions of non-Newtonian nanofluids with Reynolds model and Vogels model by means of the homotopy analysis method, Math. Comput. Modelling, 55 (2012) 1876 - 1891.

[3]. F.M.HADY, F.S.IBRAHIM, S.M.ABDEL-GAIED, M.R.EID, Boundary layer non-Newtonian flow over vertical plate in porous medium saturated with nanofluid, Appl.Math. Mech.-Engl.Ed., 32(12), 1577-1586 (2011)

[4]. Kumari Mahesh, Gorla Rama Subba Reddy, Effect of Melting on Mixed Convective Boundary Layer Flow Over a Vertical Plate Embedded in a Porous Medium Saturated with a Nanofluid, Journal of Nanofluids, Volume 4, Number 1, March 2015, pp. 82-90(9)

[5]. Rama Subba Reddy Gorla, Ali Chamkha, Abdulkareem Aloraier, Melting heat transfer in a nanofluid flow past a permeable continuous moving surface, Journal of Naval Architecture and Marine Engineering, DOI: 10.3329/jname.v8i2.6830

[6]. R.R.Kairi, Ch.RamReddy, The effect of melting on mixed convection heat and mass transfer in non-newtonian nanofluid saturated in porous medium, Frontiers in Heat and Mass Transfer (FHMT),6, 6 (2015)

[7]. R.H. Christopher, S. Middleman, Power law fluid flow through a packed tube. Ind. Eng. Chem. Fundam.4 (1965) 422 - 426.

[8]. R.V. Dharmadhikari, D.D Kale, The flow of non-Newtonian fluids through porous media. Chem. Eng.Sci. 40 (1985) 527 - 529.

D.Rajani "Heat And Mass Transfer In Non-Newtoniannanofluid Flow From A Vertical Melting Front"International Journal of Engineering Research and Applications (IJERA) , vol. 8, no.10, 2018, pp 46-53